Kinetic analysis of the spontaneous thermal polymerization of acrylic acid

Michiya Fujita [1] ・ Yu-ichiro Izato [1] ・ Atsumi Miyake [2] [*]

[1] Graduate School of Environment and Information Sciences, Yokohama National University, 79-7 Tokiwadai, Hodogaya-ku, Yokohama, Kanagawa 240-8501, Japan
[2] Institute of Advanced Sciences, Yokohama National University, 79-5, Tokiwadai, Hodogaya-ku, Yokohama 240-8501, Japan

✉ miyake-atsumi-wp@ynu.ac.jp (A. Miyake)

ABSTRACT

Acrylic acid is a monomer that has been responsible for a number of severe explosions worldwide as a result of thermal runaway. The present work was intended to lead to an improved understanding of the kinetics of the thermal polymerization and Michael addition reaction (MAR) of acrylic acid. Sealed-cell differential scanning calorimetry was carried out, and the kinetics of the thermal polymerization of acrylic acid were assessed on the basis of the model-free Friedman method. In addition, micro calorimetry using a Thermal Activity Monitor IV apparatus was conducted to determine the kinetic parameters for the MAR. The rate constant for the MAR was found to be $k\ (\text{s}^{-1}) = 3.45 \times 10^5 \times \exp\ (-9.48 \times 10^3/T\ (\text{K}))$ while the activation energy was 78.8 kJ mol^{-1}. The progress of the MAR was fitted with an *n*-order reaction model and the reaction order as well as the rate constant were determined to be linearly proportional to temperature. By employing a modified *n*-order reaction model in which the reaction order was a linear function of temperature, we obtained a reaction rate equation for the MAR that closely reproduced the experimental results over a wide temperature range.

Keywords: Acrylic acid; Thermal polymerization; Kinetic analysis; Thermal activity monitor Self accelerating polymerization temperature

1. Introduction

Acrylic acid (AA) is widely used as a feedstock for the synthesis of highly transparent and water absorptive polymers. AA polymerizes via a free-radical mechanism that is extremely exothermic when radical inhibitors or oxygen are present in insufficient quantities. Although the presence of such inhibitors can slow the radical polymerization, the exothermic Michael addition reaction (MAR), which is an ionic process, can still proceed to increase the temperature of the AA and so promote spontaneous polymerization [1]. Partly due to this phenomenon, there have been many explosions and fires attributed to the runaway reaction of

AA [2-10], and this chemical must be handled and stored on a detailed understanding of its reaction kinetics.

To understand the kinetics of the MAR, the authors have carried out isothermal tests in which AA with an excess of inhibitor was held above 120°C [11]. Based on the results of the test and the kinetics analysis assuming an n-order reaction, the reaction order was estimated to be 2.5, but this reaction rate equation could not completely reproduce the actual reaction progress of the MAR at some temperature conditions. The reaction products of the MAR have been identified by gel permeation chromatography to be at least dimeric to tetrameric AA, and in the formulation of this reaction rate equation, it must be taken into account that the reaction system consists of several AA molecules. In addition, accelerating rate calorimetry tests were conducted under the thermal runaway scenario where the spontaneous thermal polymerization initiates after the accumulation of Michael adducts, and it was found that the presence of Michael adducts increased the gas production during thermal runaway and increased the risk of tank failure [1]. Preventing thermal runaway and reducing the risk after thermal runaway of AA requires Information regarding the kinetic parameters of the MAR as well as thermal polymerization.

The kinetic parameters can allow predictions of various thermal safety parameters [12] such as the time to maximum rate (TMR), the temperature of no return (TNR) and the self accelerating decomposition/polymerization temperature (SADT/SAPT) [13]. Sheng et al. [14] conducted several calorimetric tests using milligram or gram scale samples and reported a kinetic analysis of the thermal polymerization of methyl methacrylate (MMA) with the aim of finding the SAPT. However, both stepwise calorimetric and adiabatic methods were found to be insufficiently sensitive to provide the kinetic parameters for the thermal spontaneous polymerization. In addition, the SAPT of MMA is determined by the heat generation due to thermal polymerization, while the value for AA also depends on the heat generation due to the MAR. Krause et al. [15] estimated the heat generation rate for AA polymerization via the MAR based on hot storage trials in a 1 L Dewar filled with 1 kg of stabilized AA, with the aim of determining the SAPT. Because thermal polymerization results in significant large heat generation and a rapid reaction rate, it is possible to assess this process using temperature scanning with milligram scale samples.

The construction of a suitable reaction model is particularly important for understanding the kinetics of the MAR. Although it is known that the MAR is an n-order reaction, several reaction orders have been reported and, in the vicinity of room temperature, the reaction order has been reported to be $n = 0$ [16], 1 [3] or 1.5 [17]. At relatively high temperatures (above 120 °C), a value of $n = 2.5$ [11] has been determined. Therefore, a universal reaction model for the MAR that can reproduce the correct reaction rate regardless of the temperature range is required.

Since both thermal polymerization and MAR are exothermic reactions, the kinetic analysis based on thermal analysis to capture the hear generation is very effective. Differential scanning calorimetry (DSC) offers a great potential for the determination of the kinetic parameters for chemical reactions of samples such as commodity chemicals [18], petroleum products [19, 20], food ingredients [21], and so on. DSC studies have the advantage of being very rapid and versatile. Although non-isothermal dynamic measurements are not suitable for the analysis of reactions that exhibit autocatalytic behavior with induction periods, they have the advantage over isothermal measurements of understanding the kinetics of the reaction within a reasonable measurement time [22]. The MAR generates a lesser quantity of heat and has a slower reaction rate, so such trials must be performed at extremely low temperature scanning rates using gram scale samples. The authors attempted to measure the heat release of the MAR, however, due to the very low rate of reaction, it was not possible to assess the overall heat release of the MAR [11]. Long term calorimetric test, such as several months, are required to fully measure the heat release of the MAR.

The aim of the present work was to obtain a better understanding of the kinetics of the thermal polymerization and the MAR of AA. In this work, sealed-cell differential scanning calorimetry (SC-DSC) was used to analyze the kinetics of the self-initiation and the thermal polymerization processes. In addition, micro calorimetry using a Thermal Activity Monitor IV was employed to estimate the kinetic parameters of the MAR. The model-free Friedman method and model-fitting employing an *n*-order reaction system were used to process the data.

2. Experimental

2.1 Materials

Two types specimens were prepared. These were AA containing 200 ppm of the radical inhibitor *p*-methoxyphenol, obtained from Kanto Chemical, and AA containing *p*-methoxyphenol at 2 wt%. The latter sample is referred to as AAMQ in this study.

2.2 Kinetic analysis of thermal polymerization

An HP DSC827^e instrument (Mettler Toledo) was used to acquire SC-DSC data. In each trial, a 3 mg quantity of AA was placed in an aluminum cell and the sell was then sealed. The specimens were heated from 50 to 500 °C at rates of 0.5, 1, 2 or 4 K min^{-1}. The apparatus was calibrated for temperature and heat flow based on the melting of high-purity indium (99.99%). The AKTS Thermo-kinetic software package [23] was used for kinetic modeling.

2.3 Kinetic analysis of the Michael addition reaction

In order to obtain data regarding the MAR (which generates only a small amount of heat

and has a slow reaction rate) within a reasonable time span, non-isothermal analyses were performed using extremely low heating rates. These trials employed a Thermal Activity Monitor apparatus (TAM IV, TA Instruments) that combines high sensitivity with long term temperature stability. In each experiment, a 3 g quantity of AAMQ was transferred into a glass vial which was then placed in a stainless steel sample holder, as shown in Fig. 1. The heating range was from 60 to 150 °C, and the heating rates were at 25, 50, 100 or 200 mK h^{-1}, with a detection limit of 2 µW. Using these conditions, more than three months were required to complete the test at a heating rate of 25 mK h^{-1}.
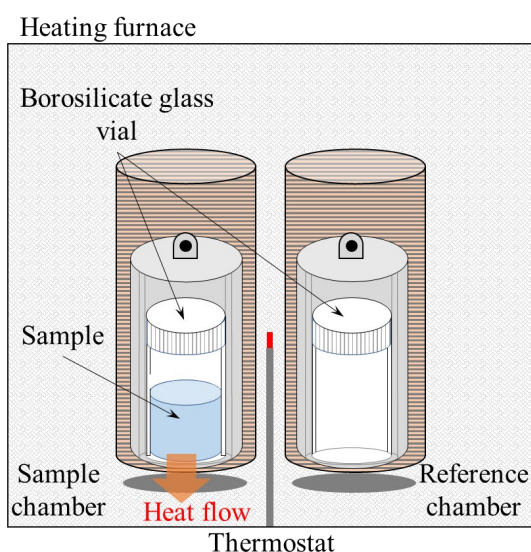

Figure 1. A diagram of the TAM IV apparatus.

3. Results and discussion

3.1 Kinetic analysis of thermal polymerization

Figure 2 presents the SC-DSC results. A single exothermic peak due to thermal polymerization was observed at all four heating rates and the average heat release was 1.1 kJ g^{-1}. The kinetic analysis in this session was based on the model-free Friedman method [24-29] and the reaction progress, α, was determined from the equation (1):

$$\alpha(T) = \frac{\int_{T_0}^{T}\big(S(T) - B(T)\big)\mathrm{d}T}{\int_{T_0}^{T_f}\big(S(T) - B(T)\big)\mathrm{d}T} \tag{1}$$

The radical inhibition reaction was considered to have started at the same time as the heat flow during these trials and before the appearance of the exothermic peak. Consequently, it was assumed that a slight exotherm occurred due to this process and the reaction progress was defined as shown in Fig. 3. One possible approach to the evaluation of the kinetic parameters,

4

particularly E_a and A, involves the model-free Friedman method. Based on the Arrhenius equation, the logarithm of the conversion rate, $d\alpha/dt$, as a function of the reciprocal temperature, $1/T(t_\alpha)$, at any α can be expressed as:

$$\ln\left(k(T)f(\alpha)\right) = \ln\left(\frac{d\alpha}{dt}\right) = \ln\left(A(\alpha)f(\alpha)\right) - \frac{E_a(\alpha)}{RT(t_\alpha)} \tag{2}$$

In the present work, a plot of the logarithm of $d\alpha/dt$ against $1/T(t_\alpha)$ produced a straight line, for which the slope equaled $-E_a(\alpha)/R$ and the intercept on the y-axis equaled $\ln(A(\alpha)f(\alpha))$. The variations in $E_a(\alpha)$ and $A(\alpha)f(\alpha)$ with α were ascertained using a dynamic technique, as E_a can be determined without knowing $f(\alpha)$ by this method. The heat flow during each DSC trial was calculated based on the normalized reaction rate, $d\alpha/dt$, and the average heat value of the thermal polymerization of AA under non-isothermal conditions as shown in Fig. 2 (dashed line). The calculated heat flow curves generated in this manner were found to be in good agreement with the experimental results at each heating rate. We estimated E_a and $\ln(A(\alpha)f(\alpha))$ values based on this predicted reaction rate and Eq. (2), and the results are provided in Fig. 4. The dynamic changes of E_a with respect to the reaction progress indicate that this exothermic behavior involved multiple reaction processes, such as initiation, inhibition by the radical inhibitor [30-32], propagation and termination (as summarized in Fig. 5) as well as a gel effect [33-35]. From these results, it is possible to estimate the temperature rise profile due to the spontaneous thermal polymerization of AA under adiabatic conditions, but its validity needs to be verified by actual adiabatic tests.
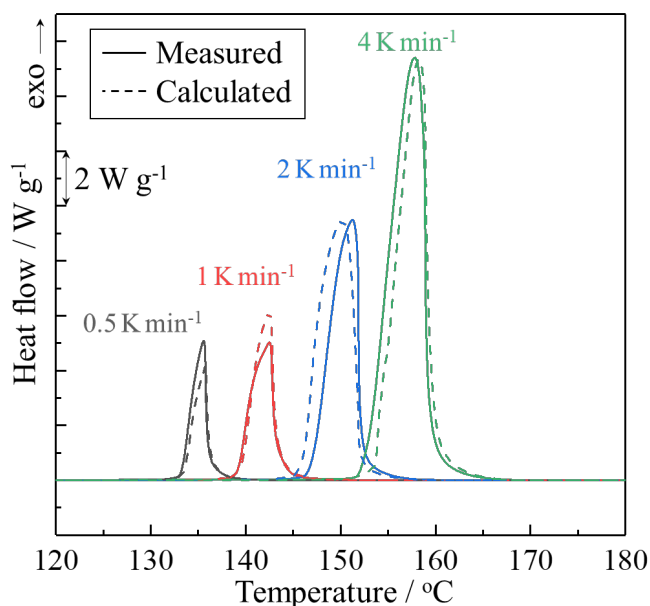

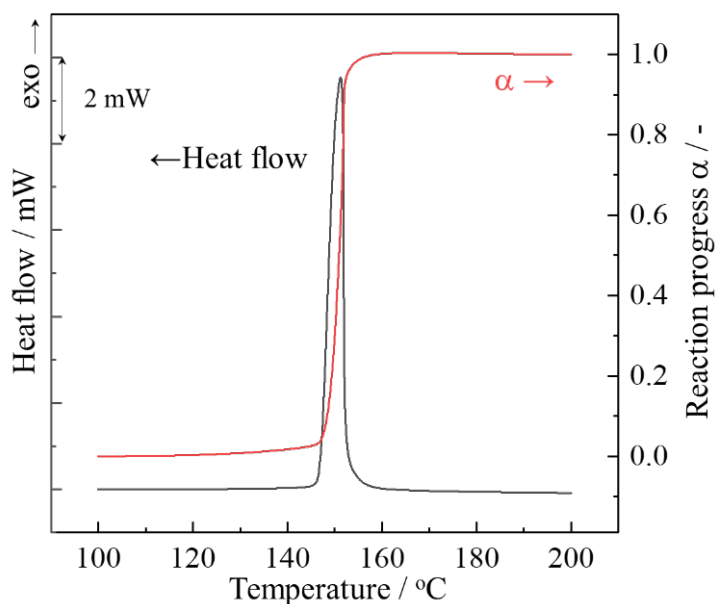Figure 2. SC-DSC curves obtained from AA at heating rates of 0.5, 1, 2, or 4 K min^{-1}.

Figure 3. The definition of reaction progress based on heat flow during SC-DSC.
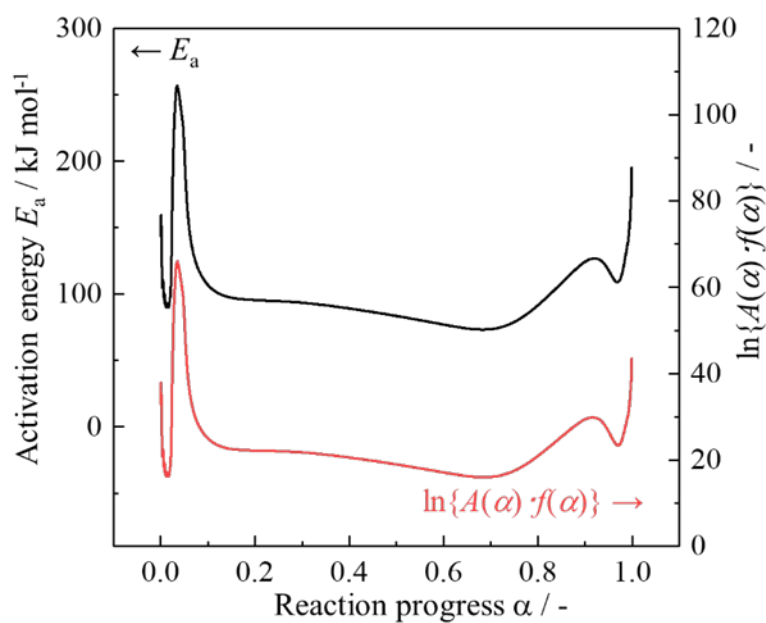

Figure 4. The activation energy, E_a, and pre-exponential factor term (expressed as $\ln\{A(\alpha)f(\alpha)\}$ as determined using the model-free Friedman method) for the thermal polymerization of AA as functions of the reaction progress.
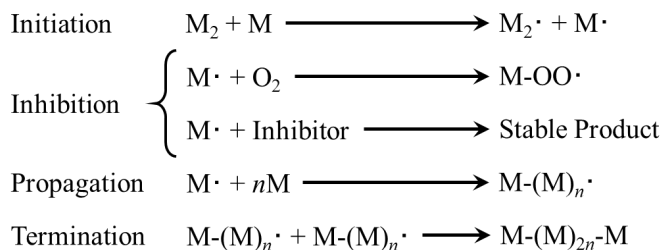
Initiation	$M_2 + M \longrightarrow M_2\cdot + M\cdot$
Inhibition	$\begin{cases} M\cdot + O_2 \longrightarrow M\text{-}OO\cdot \\ M\cdot + \text{Inhibitor} \longrightarrow \text{Stable Product} \end{cases}$
Propagation	$M\cdot + nM \longrightarrow M\text{-}(M)_n\cdot$
Termination	$M\text{-}(M)_n\cdot + M\text{-}(M)_n\cdot \longrightarrow M\text{-}(M)_{2n}\text{-}M$

Figure 5. A summary of the processes occurring during the thermal polymerization of AA ($M\cdot$ = monomer radical).

3.2 Kinetic analysis of the Michael addition reaction

Figure 6 presents the results acquired from the micro calorimetry analyses of AAMQ using the TAM IV instrument. A heat generation of approximately 80 J g^{-1}, which is considered to represent the heat of the MAR, was observed at each heating rate. The progress of the MAR was calculated using the model-free Friedman method and the exothermic behavior was simulated, as shown in Fig. 6 (dashed line). The simulation curve is seen to have reproduced the experimental results well, and so a rate equation that allows the reaction progress at any temperature to be calculated could be conditioned was obtained. Figure 7 presents the E_a and $\ln(A(\alpha)f(\alpha))$ values determined using Eq. (2), while Figure 8 shows the predicted reaction progression at 90, 100, 110, 120, and 130 °C based on the model-free Friedman equation. The construction of an appropriate reaction model is particularly important to understanding the kinetics of the MAR. For the MAR, we tried to apply a specific reaction model to calculate the reaction rate. In this regard, E_a, A, and the reaction model, $f(\alpha)$, are related according to the equation [22, 36]:

$$\ln\left(\frac{d\alpha}{dt}\right) = \ln A - \frac{E_a}{RT} + \ln f(\alpha) \tag{3}$$

where, for an *n*-order reaction model, we have:

$$f(\alpha) = (1 - \alpha)^n \tag{4}$$

Combining Eq. (3) and (4) gives:

$$\ln\left(\frac{d\alpha}{dt}\right) = \ln A - \frac{E_a}{RT} + n\ln(1 - \alpha) \tag{5}$$

All three values were calculated by fitting the reaction progress data using the *n*-order reaction model, and the fitting results are presented in Fig. 8. Figure 9 provides the Arrhenius plot for the MAR and the calculated reaction orders, *n*, based on fitting at each temperature. This value

was found to be directly proportional to temperature. These results indicate that n was correlated with the number of molecules in the reaction system. Because the MAR is a multi-step addition reaction during which monomers continually add to form dimers, trimers, and larger molecules, the number of reacting monomers increased with increasing temperature. Assuming a single-step reaction, n should be constant, although the present data demonstrate that n was a function of temperature. From these results, the rate of the MAR was estimated as:

$$\frac{\mathrm{d}\alpha}{\mathrm{d}t} = A \exp\left(-\frac{E_\mathrm{a}}{RT}\right) \times (1-\alpha)^n$$

$$= 3.45 \times 10^5 \times \exp\left(-\frac{7.88 \times 10^4}{RT}\right) \times (1-\alpha)^{3.0-\frac{750}{T}}$$

(6)

The activation energy and the pre-exponential factor were calculated to be 78.8 kJ mol^{-1} and 3.45×10^5 s^{-1} respectively. Figure 10 presents a comparison between the experimental values acquired during the micro calorimetry trials and the heat flows calculated using Eq. (6). The calculated values indicate that the reaction rate increased at lower temperatures than are seen in the experimental data. This discrepancy can be explained by considering that the MAR is known to proceed at an extremely slow rate even near room temperature, whereas, in the micro calorimetry experiments, the measurements were started at 60 °C so as to reduce the length of time required to acquire data It should be possible to estimate the reaction rate at 60 °C or lower by extrapolation from data acquired above this temperature. It is also evident from this figure that the calculated values accurately reproduced the peak top temperatures at each heating rate in the experimental data.

The improvement of the formulation for reaction rate of the MAR by the modified n-order model Eq. (6) in the present study is demonstrated by comparing previous n-order models, including the reaction rate equation for the MAR in Eq. (7) below, calculated in our previous study [11]:

$$\frac{\mathrm{d}[\mathrm{AA}]}{\mathrm{d}t} = 2.41 \times 10^8 \times \exp\left(-\frac{1.18 \times 10^5}{T}\right) \times [\mathrm{AA}]^{2.5}$$

(7)

Figure 11 presents a comparison of measured changes in AA concentration at 120, 125, 130, and 135°C [11] with calculations based on the MAR reaction rate equations including the modified n-order model in Eq. (6) and the previous n-order models [3, 15-17]. The AA concentration change was calculated by assuming that [AA] = 1-α for the relationship between AA concentration and the reaction progress α of MAR. The modified n-order model in Eq. (6) reproduces the measured values better than previous n-order models. Eq. (7) also replicates the measurements well, but since Eq. (7) was obtained based on fitting from these measured values, it is not surprising that they match. Figure 12 presents the calculation results of heat flow at heating rates of 25, 50, 100, and 200 mK h^{-1} calculated by Eqs. (6) and (7). It can be seen that Eq. (7) of the 2.5th order model does not reproduce the experimental results of non-isothermal

dynamic processes. These results indicate that equation (6) more faithfully reproduces the actual progress of MAR under diverse temperature conditions than the previous models.
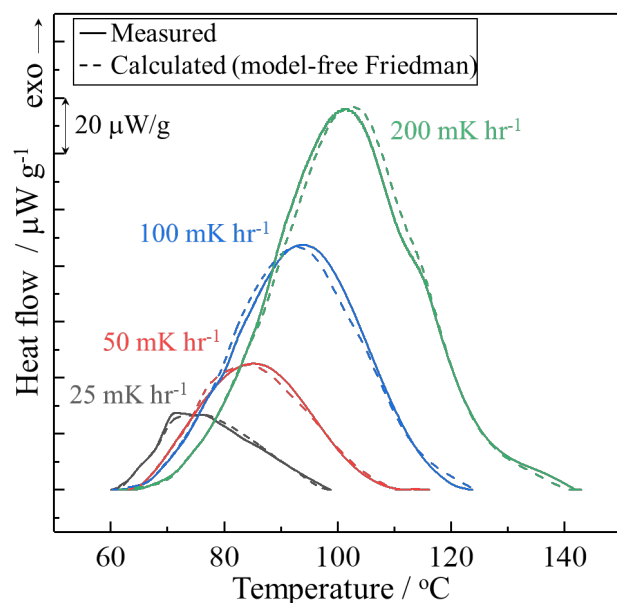

Figure 6. The results of micro calorimetry analyses of the MAR using a TAM IV instrument together with heat flow simulations based on the model-free Friedman method.
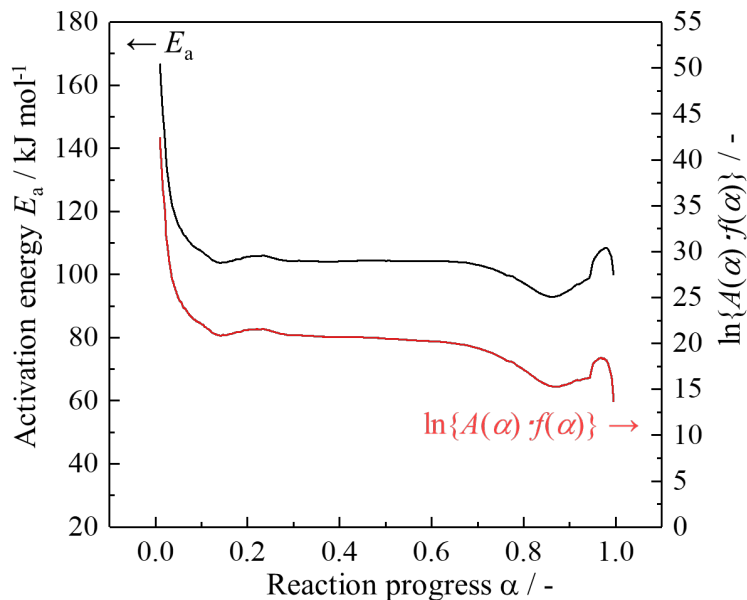

Figure 7. The activation energy, E_a, and pre-exponential factor term (expressed as $\ln\{A(\alpha)f(\alpha)\}$ as determined using the model-free Friedman method) for the MAR as functions of the reaction progress.
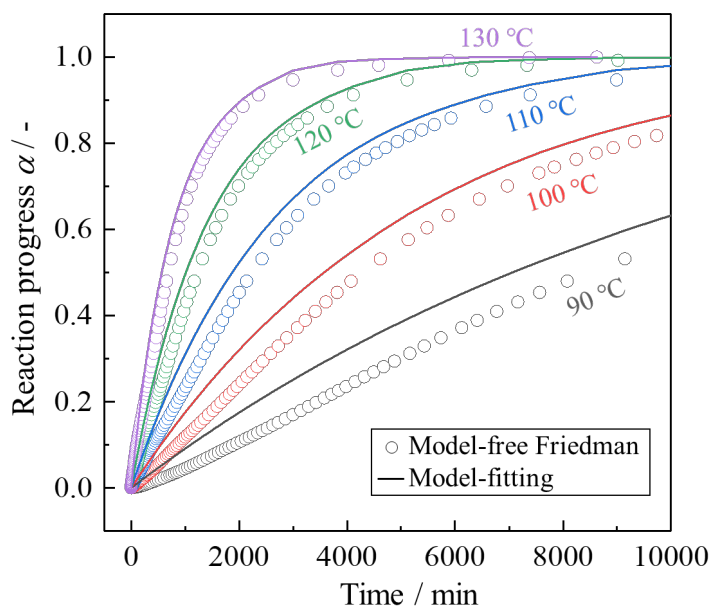
Figure 8. Predicted MAR progressions at several temperatures based on the model-free Friedman method and the n-order reaction model-fitting method.
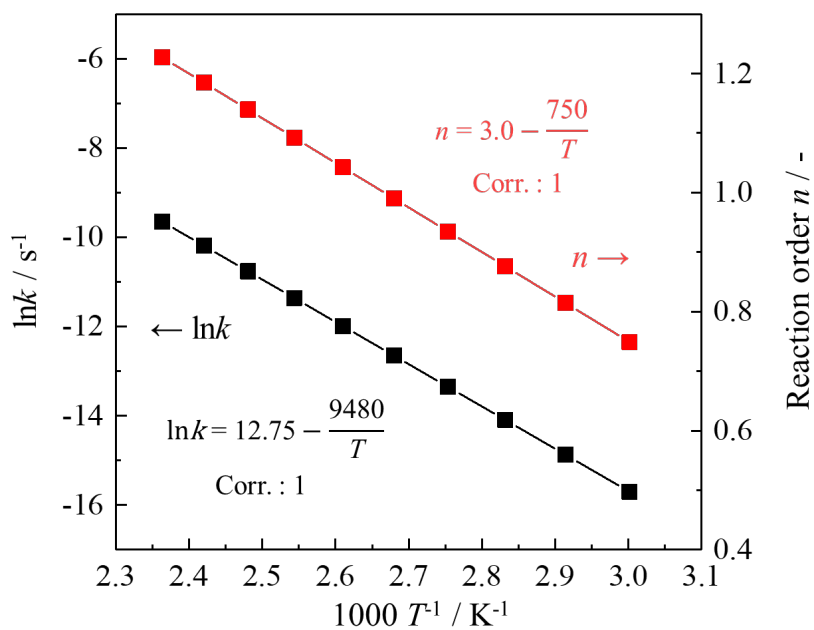

Figure 9. An Arrhenius plot for the MAR and the reaction orders at multiple temperatures as calculated by the n-order reaction model-fitting method (Corr. = correlation coefficient)
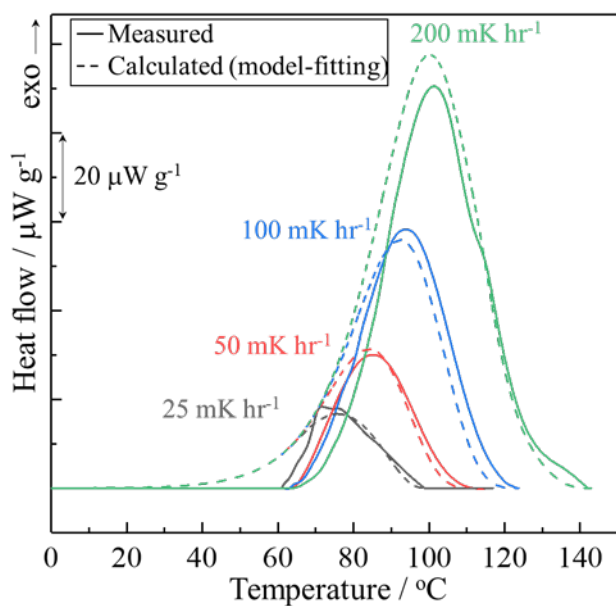
Figure 10. A comparison between experimental results from micro calorimetry and the calculated heat flows obtained using Eq. (6).
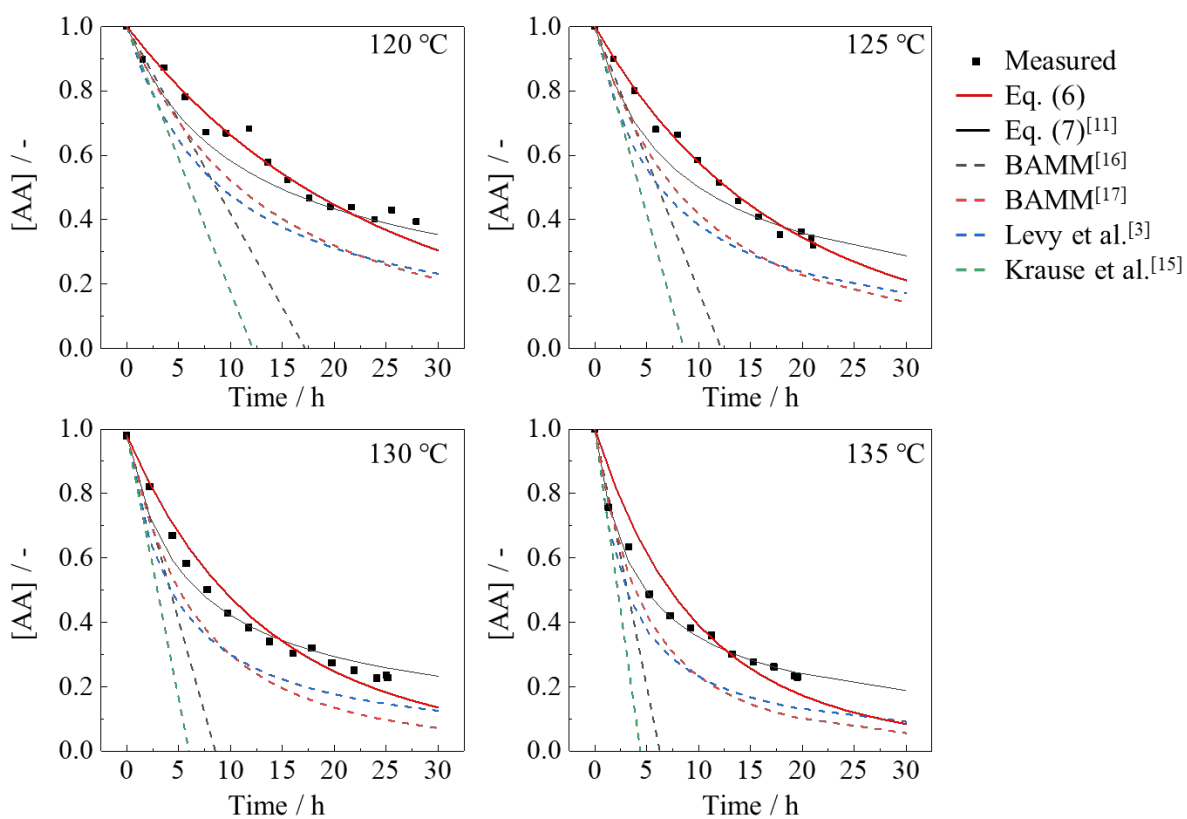

Figure 11. A comparison of measured changes in AA concentration at 120, 125, 130, and 135°C with calculations based on the MAR reaction rate equations
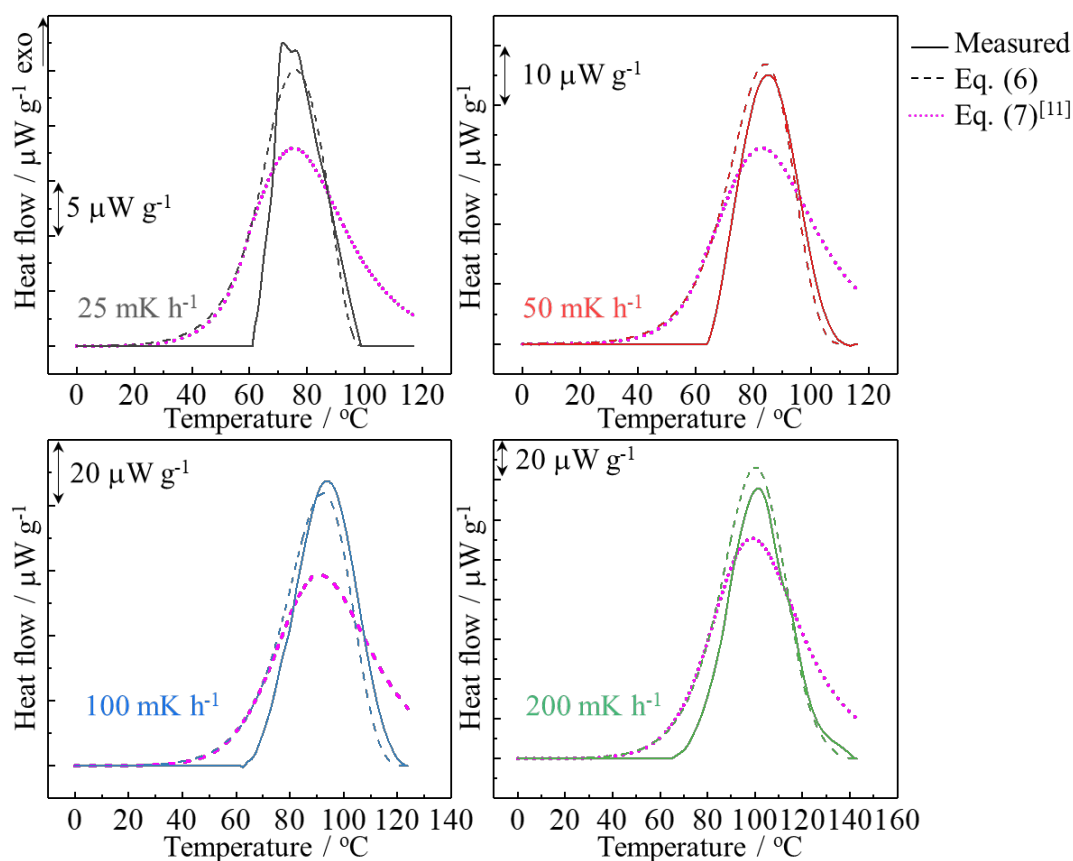
Figure 12. Comparison of heat flow at heating rates of 25, 50, 100, and 200 mK h^{-1} calculated by Eqs. (6) and (7)

4. Conclusions

The present study performed a kinetic analysis of the spontaneous thermal polymerization and the MAR of AA.

The model-free Friedman method was found to provide accurate predictions of the thermal polymerization of stabilized AA under non-isothermal conditions. This kinetic analysis allowed simulations of the reaction progress based on SC-DSC results. The thermal polymerization process was predicted by defining the progress of the reaction, including a slight exotherm attributed to the radical inhibition reaction. If the model-free Friedman method can be used to separately analyze the data for each reaction, non-isothermal SC-DSC results are sufficient to permit an investigation of the kinetics of AA thermal polymerization.

The kinetic parameters for the MAR were determined based on the use of a fitting method in conjunction with a modified n-order reaction model in which n is a linear function of temperature. The resulting values for A, E_a, and $n(T)$ were 3.45×10^5 s^{-1}, 78.8 kJ mol^{-1}, and $3.0 - 750/T$. The rate equation for the MAR was also determined to accurately reproduce the actual rates over a wide temperature range. Based on this modified n-order reaction rate equation,

which is better than the conventional models, it is expected to contribute to the control MAR and the safe or optimal handling of AA in the chemical industries.

Nomenclature

A	Pre-exponential factor (s^{-1})
B	Baseline signal for heat flow in calorimetry (W g^{-1})
E_a	Activation energy (kJ mol^{-1})
$f(\alpha)$	Reaction model (-)
K	Reaction rate constant (s^{-1})
N	Reaction order (-)
R	Gas constant (J mol^{-1} K^{-1})
S	Heat flow signal in calorimetry (W g^{-1})
T	Time (s or min or h)
t_α	Time at which the reaction progress is α (s)
T	Temperature (°C or K)
T_0	Initial temperature (°C or K)
T_f	Final temperature (°C or K)

Greek letters

α	Reaction progress, conversion (-)

References

[1] Fujita M, Izato Y, Iizuka Y, Miyake A. Thermal hazard evaluation of runaway polymerization of acrylic acid, Process Saf Environ Prot. 2019;129:339-347.

[2] Center for Chemical Process Safety (CCPS). Guidelines for safe storage and handling of reactive materials. New York: American Institute of Chemical Engineers; 1995.

[3] Levy LB, Penrod JD. The anatomy of an acrylic acid runaway polymerization, Plant/Operation Prog. 1989;8:105-108.

[4] Nippon Shokubai Co., Ltd. Himeji plant explosion and fire at acrylic acid production facility investigation report. Nippon Shokubai Co., Ltd. Japan. 2013. https://www.shokubai.co.jp/en/news/file.cgi?file=file1_0071.pdf of subordinate document. Accessed 22 Apr 2020.

[5] Kao C, Hu K. Acrylic reactor runaway and explosion accident analysis. J Loss Prev Proc Ind. 2002;15:213-222.

[6] Kalfas G, Krieger T, Wilcox R. Improvements in the safety screening of resin manufacturing processes. Proc Safe Prog. 2009;28:275-281.

[7] Gromacki M. Acrylic polymer reactor accident investigation: Lessons learned and three years later. CCPS International Conference and Workshop on Process Industry Incidents. USA. 2000.

[8] Kurland JJ, Bryant DR. Shipboard polymerization of acrylic acid. Plant/Operation Prog. 1987;6:203-207.

[9] Gustin JL. How the study of accident case histories can prevent runaway reaction accidents from recurring. Inst of Chem Eng. 2002;80:16-24.

[10] Wang C, Chang C, Tseng J. Epoxy acrylic resin experimental analysis of runaway reaction. J Therm Anal Calorim. 2019;138:2839-2851.

[11] Fujita M, Iizuka Y, Miyake A. Thermal and kinetic analyses on Michael addition reaction of acrylic acid. J Therm Anal Calorim. 2017;128:1227–1233.

[12] Sun Q, Jiang L, Li M, Sun J. Assessment on thermal hazards of reactive chemicals in industry: State of the art and perspectives. Prog Energy Combust Sci. 2020; https://doi.org/10.1016/j.pecs.2020.100832

[13] UN Model Regulations. United Nations Recommendations on the transport of dangerous goods - model regulations, 19th rev. New York, Geneva: United Nations; 2015.

[14] Sheng M, Dan F, Horsch S, Bellair R, Holsinger M, Scholtz T, Weinberg S, Sopchik A. calorimetric method to determine self-accelerating polymerization temperature (SAPT) for monomer transportation regulation: kinetics and screening criteria. Org Process Res Dev. 2019;23:737−749.

[15] Krause G, Wehrstedt K, Malow M, Budde K, Mosler J. Safe transport of acrylic acid in railroad tank cars, part 1: Determination of the self-accelerating decomposition temperature. Chem Eng Technol. 2014;37:1460−1467.

[16] Rohm and Haas Company. Storage and handling of acrylic and methacrylic esters and acids. Philadelphia: Rohm and Haas Brochure; 1987.

[17] Basic Acrylic Monomer Manufacturers Inc. Acrylic acid, a summary of safety and handling, 4th ed. Basic Acrylic Monomer Manufacturers Inc. USA 2013. http://msdssearch.dow.com/publishedliteraturedowcom/dh_0933/0901b80380933166.pdf of subordinate document. Accessed 22 Apr 2020.

[18] Torfs JC, Deij L, Dorrepaal AJ, Heijens JC. Determination of Arrhenius kinetic constants by differential scanning calorimetry. Analytical Chemistry. 1984:56;2863-2867.

[19] Khoshooei MA, Fazlollahi F, Maham Y. A review on the application of differential scanning calorimetry (DSC) to petroleum products. J Therm Anal Calorim. 2019:138;3455-3484.

[20] Kök M, Iscan A. Oil shale kinetics by differential methods. J Therm Anal Calorim. 2007:88;657-661.

[21] Smith KW, Cain FW, Talbot G. Kinetic analysis of nonisothermal differential scanning calorimetry of 1, 3-dipalmitoyl-2-oleoylglycerol. J Agric Food Chem. 2005:53;3031-3040.

[22] Vyazovkin S, Burnham AK, Criado JM, Pérez-Maqueda LA, Popescu C, Sbirrazzuoli N. ICTAC Kinetics Committee recommendations for performing kinetic computations on thermal analysis data. Thermochim Acta. 2011;520:1-19.

[23] AKTS. Advanced Kinetics and Technology Solutions. https://www.akts.com of subordinate document. Accessed 22 April 2020.

[24] Friedman HL. Kinetics of thermal degradation of char-forming plastics from thermogravimetry. Application to a phenolic plastic. J Polym Sci C. 1963;6:183–95.

[25] Ozawa T. Applicability of Friedman plot. J Thermal Anal. 1986;3:547–51.

[26] Bercic G. The universality of Friedman's isoconversional analysis results in a model-less prediction of thermodegradation profiles. Thermochim Acta. 2017;650:1–7.

[27] Izato Y, Miyake A. Kinetic analysis of the thermal decomposition of liquid ammonium nitrate based on thermal analysis and detailed reaction simulations. J Therm Anal Calorim. 2018;134:813-823.

[28] Mizuta R, Izato Y, Miyake A. Thermal ignition behavior of waste woods mixed with unsaturated fatty acids. J Therm Anal Calorim. 2015;121:361-369.

[29] Yamamoto Y, Miyake A. Influence of a mixed solvent containing ionic liquids on the thermal hazard of the cellulose dissolution process. J Therm Anal Calorim. 2017;27:743-748.

[30] Hartwig A., Brand RH, Pfeifer C, Dürr N, Drochner A, Vogel H. Safety and quality aspects of acrylic monomers. Macromol Symp. 2011;302:280−288.

[31] Levy LB. Inhibition of acrylic acid polymerization by phenothiazine and p-methoxyphenol. II. Catalytic inhibition by phenothiazine. J Polym Sci Part A: Polym Chem. 1992;30:569−576.

[32] Kirch LS, Kargol JA, Magee JW, Stuper WS. Stability of acrylic monomers. Plant/Oper Prog. 1988;7:270−274.

[33] Maschio G, Moutier C. Polymerization reactor: The influence of "gel effect" in batch and continuous solution polymerization of methyl methacrylate. J Appl Polym Sci. 1989;37:825−840.

[34] Chiu WY, Carratt GM, Soong DS. A computer model for the gel effect in free-radical polymerization. Macromolecules 1983;16:348−357.

[35] Verros GD, Achilias DS. Modeling gel effect in branched polymer systems: Free-radical solution homopolymerization of vinyl acetate. J Appl Polym Sci. 2009;111:2171-2185.

[36] Ding J, Yu L, Wang X, Xu Q, Yang S, Ye S, Jiang J. A kinetic-based approach in accelerating rate calorimetry with the varying thermal inertia consideration. J Therm Anal Calorim. 2019; https://doi.org/10.1007/s10973-019-09081-z